Czech Technical University in Prague

Faculty of Mechanical Engineering

Department of Mechanics, Biomechanics and Mechatronics

Doctoral thesis statement

Finite element method based computational time reversal in elastodynamics

Michal Mračko

Branch of Study: Mechanical Engineering

Ph.D. Programme: Mechanics of Solids, Deformable Bodies and Continua

Supervisor: Ing. Jiří Plešek, CSc.

Doctoral thesis statement for obtaining the academic title of "Doctor", abbreviated to "Ph.D."

Prague March 2023

Title in Czech: Řešení úloh časové reverzace v elastodynamice použitím metody konečných prvků

The doctoral thesis was produced in full-time manner of Ph.D. study at the Department of Mechanics, Biomechanics and Mechatronics of the Faculty of Mechanical Engineering of the CTU in Prague.

Candidate: Ing. Michal Mračko
Department of Mechanics, Biomechanics and Mechatronics
Technická 1902/4
CZ-16636 Prague 6

Supervisor: Ing. Jiří Plešek, CSs.
Institute of Thermomechanics of the Czech Academy of Sciences
Dolejškova 1402/5
CZ-18200 Prague 8

Supervisor-Specialist: doc. Ing. Radek Kolman, Ph.D.
Institute of Thermomechanics of the Czech Academy of Sciences
Dolejškova 1402/5
CZ-18200 Prague 8

Opponents:

The doctoral thesis statement was distributed on: .....
The defense of the doctoral thesis will be held on ..... at ..... a.m./p.m. in the conference room no. 17 (ground floor), Faculty of Mechanical Engineering of the CTU in Prague, Technická 4, Praha 6 before the Board for the Defense of the Doctoral Thesis in the branch of study Mechanical Engineering.
Those interested may get acquainted with the doctoral thesis concerned at the science and research department of the Faculty of Mechanical Engineering of the CTU in Prague, Technická 2, Prague 6.

Prof. Ing. Michael Valášek, Dr.Sc.

Chairman of the board of the field Mechanics of Solids, Deformable Bodies and Continua

Faculty of Mechanical Engineering of the CTU in Prague

Abstract

The aim of this thesis is to develop a methodology to correctly reconstruct the source in the time domain using the computational time reversal method. This capability would allow identification of existing or forming flaws in the material by analyzing the reconstructed signals. Localization of sources using refocusing of energy is a well-established method, but reconstruction of these sources is still an unsolved problem. A dedicated explicit solver based on the finite element method is developed to solve the elastic wave propagation in solid material. The developed methodology is numerically tested and also verified using experimental data. It is proved that the reconstruction is feasible and correct with a tuned model. Thanks to the presented research, the practical deployment of the computational time reversal method is more promising and it can be included in the concept of the so-called digital twin. On the other hand, the method is very sensitive to the input parameters and very computationally demanding, which are aspects that open up possibilities for further research.

Keywords: Time reversal, source reconstruction, finite element method

Abstrakt

Cílem práce je vyvinout metodologii pro věrohodnou rekonstrukci zdroje v časové oblasti za použití metody výpočetní časové reverzace. Tato schopnost by pomocí analýzy rekonstruovaných signálů umožnila identifikovat stávající nebo vznikající poruchy v materiálu. Lokalizace zdroje pomocí zpětného zaměření energie je známá metoda, ale rekonstrukce časového průběhu zdroje je stále otevřený problém. Pro řešení šíření elastických vln byl vyvinut explicitní řešič založený na metodě konečných prvků. Vyvinutá metodologie byla otestována numericky a verifikována na experimentálních datech. Bylo prokázáno, že s naladěným numerickým modelem je rekonstrukce zroje proveditelná a správná. Díky provedenému výzkumu je praktické nasazení metody časové reverzace perspektivnější a metoda může být zahrnuta do konceptu zvaného digitální dvojče. Metoda je však velmi citlivá na vstupní parametry a náročná na výpočet, což otevírá možnosti pro další výzkum.

Klíčová slova: Časová reverzace, rekonstrukce zdroje, metoda konečných prvků

Contents

1 Introduction

With the advent of Industry 4.0, [21, 22], terms such as structural health monitoring (SHM), [23, 24, 25], or digital twin, [26, 27], have been more frequently cited. Knowing the structural changes in a construction caused by emerging flaws is as attractive as knowing the end of life of working equipment or consumables. This inevitably requires real-time monitoring and evaluation of the recorded data. One possible way to evaluate this is through a computational model - the digital twin. The correct and robust localization of cracks and defects in bodies and structures in energetics [28], civil engineering [29], or aerospace [30], is still a hot topic despite the long history of this research. Moreover, this knowledge and information about cracks are needed for practical applications to ensure safe operation in various industries, such as power plants, aircraft, vehicles, satellites, and many others.

One method for locating flaws in structures is the time reversal (TR) method. The TR method belongs to the family of inverse methods in physics, [31], and is based on the properties of the Hamiltonian system [32]. The TR method is a powerful tool that can be used in various physical fields involving wave propagation. It uses the property of reversibility of wave propagation to focus the energy to the original source location in space and time. When the original source is very local, this procedure is called refocusing. Nowadays, the most important applications are in nondestructive testing (NDT), underwater acoustics [33, 34], biomedical ultrasound imaging [35], surgery and lithotripsy [36, 37], and last but not least, seismology [38]. In ultrasonic NDT, the TR method can be used to detect defects in materials and cracks in bodies.

The computational TR method has been widely employed, e.g. to localize scaterrers [39, 40, 41], to identify damage in a beam structure [42], to reconstruct the shape of traction-free scaterrers [43], or to localize noise sources in a road vehicle [44]. Several works are dedicated to investigate or improve the quality of reconstruction of the original source [45, 46, 47]. While localization is a mastered process, reconstruction of the source in the time domain has not yet been fully managed and a methodology to perform the TR in standard and widely used numerical methods such as the finite element method (FEM) has not been fully established. This work aims to improve the reconstruction of the exciting signal in the time domain and to determine the proper procedure for deploying TR in practice, i.e., in commercial finite element (FE) software.

2 State of the art

2.1 Time reversal method

In practice, the process of localization is accomplished in two steps. The first step, based on forward propagation, is the measurement on a real structure. In the second step, the measured signals are reversed in time and transmitted to the computational model, where, based on backpropagation, the energy is focused into the location of the original source. The mentioned process is schematically shown in Figure 1. Generally, one works only with partial information (incomplete data from sensors), since it is not possible to record response signals in the whole structure. There are two approaches to perform effective refocusing using the TR method. The first is using a substantial number of transducers in combination with a short recording time (and computation time), the second is the exact opposite – using only one or several transducers combined with a long recording time. The second approach exploits reflections at the structure boundaries, which compensate for the lack of direct information and overall create a virtual time-reversal mirror, see [48].

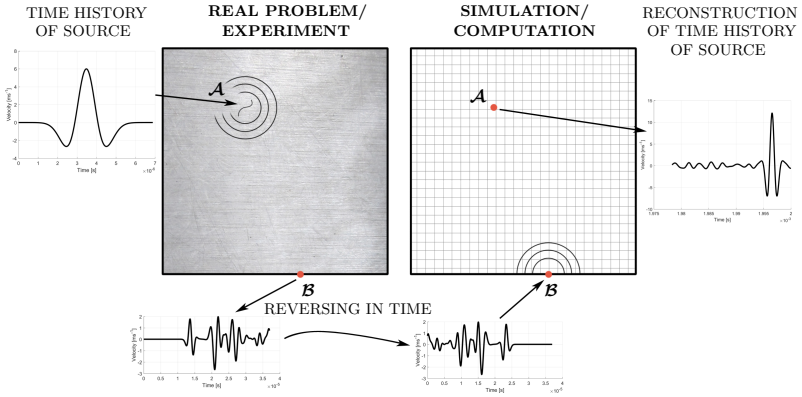

Figure 1: *Application of TR method in NDT.*

2.2 TR problem - definitions and governing equations

In this work, the classical theory of small deformations of elastic isotropic media is used for the mathematical description of elastic wave propagation in solids, which is applied to the frontal and reverse problem of TR. The definition of the problem was inspired by [49].

2.2.1 Definition of the frontal problem

The first step is to define the frontal problem with appropriate boundary and initial conditions. An open bounded domain $\Omega \in \mathbb{R}^3$ with smooth boundary $\partial\Omega$ is considered. Moreover, the linear equations of elastodynamics in the domain Ω and in time $t \in [0, T]$ are considered. The governing equations of elastodynamics, see [50], are given by the kinematic relation, the Hooke's law, and the Cauchy's equation without volume force as

$$\nabla \cdot \boldsymbol{\sigma} = \rho \ddot{\boldsymbol{u}}, \quad \boldsymbol{\sigma} = \boldsymbol{C} \colon \boldsymbol{\varepsilon}, \quad \boldsymbol{\varepsilon} = \frac{1}{2}(\nabla \boldsymbol{u} + (\nabla \boldsymbol{u})^{\intercal}), \quad 0 \leq t \leq T, \quad \boldsymbol{x} \in \Omega, \tag{1a}$$

with boundary conditions

$$\mathbb{B}\boldsymbol{u} = \boldsymbol{0} \text{ on } \partial\Omega, \tag{1b}$$

and with initial conditions

$$\boldsymbol{u}(\boldsymbol{x}, t = 0) = \boldsymbol{u}^0(\boldsymbol{x}), \quad \dot{\boldsymbol{u}}(\boldsymbol{x}, t = 0) = \boldsymbol{v}^0(\boldsymbol{x}) \quad \boldsymbol{x} \in \Omega. \tag{1c}$$

In the aforesaid relations, the superimposed dots, $\dot{\square}$, $\ddot{\square}$, denote the derivatives with respect to time t and the operator $\nabla = \{\frac{\partial}{\partial x_1}, \frac{\partial}{\partial x_2}, \frac{\partial}{\partial x_3}\}$, $\boldsymbol{\sigma}$ is the Cauchy stress tensor, $\boldsymbol{\varepsilon}$ is the infinitesimal strain tensor, $\boldsymbol{C}$ is the elastic tensor, and ρ is the mass density. Furthermore, $\boldsymbol{u}(\boldsymbol{x}, t)$ is the displacement, $\dot{\boldsymbol{u}}(\boldsymbol{x}, t)$ is the velocity, and $\ddot{\boldsymbol{u}}(\boldsymbol{x}, t)$ is the acceleration. For isotropic elastic medium, we consider the Hooke's law as $\boldsymbol{\sigma} = \Lambda \operatorname{tr}(\boldsymbol{\varepsilon})\mathbf{I} + 2G\boldsymbol{\varepsilon}$, where Λ and G are Lamé's constants.

Furthermore in (1b), $\mathbb{B}$ is a boundary operator on the displacement field $\boldsymbol{u}(\boldsymbol{x}, t)$ as the operator imposing boundary conditions on $\Gamma = \partial\Omega$. Neumann boundary conditions as stress-free boundary conditions are prescribed on Γ_{N} and Dirichlet boundary conditions are prescribed on

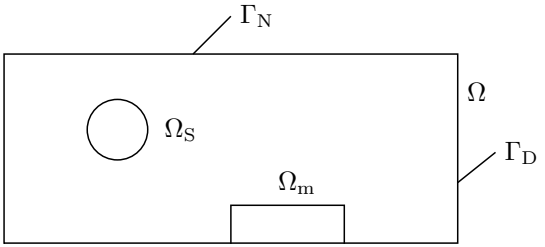

Figure 2: *Scheme of TR problem. Ω is the the domain of interest, Ω_S is the support of the original source, and Ω_m is the area of measurement.*

Γ_D, where $\Gamma_D \cup \Gamma_N = \Gamma$ and $\Gamma_D \cap \Gamma_N = 0$. The initial conditions are given by the displacement field $\boldsymbol{u}^0(\boldsymbol{x})$ and the velocity field $\boldsymbol{v}^0(\boldsymbol{x})$ at initial time $t = 0$ as in (1c). In future text, notations such as $\boldsymbol{u}(\boldsymbol{x}, t)$, $\boldsymbol{u}^t(\boldsymbol{x})$, and $\boldsymbol{u}^t$ are equivalent.

The relations (1c) represent an initial condition and we assume that $\boldsymbol{u}^0$ and $\boldsymbol{v}^0$ have a support in $\Omega_S \subset \Omega$, which is only local, i.e., the region Ω_S is much smaller than the whole domain Ω. In general, we obtain the displacement field $\boldsymbol{u}(\boldsymbol{x}, t)$ as a solution of the problem defined in (1).

In this work, the frontal problem numerically simulates the real measurement on a real structure, usually the time history of some displacement or velocity components. Here, the experimental data are replaced by the record of the response of the FE model. During the frontal problem, we record the time history of the velocity $\dot{\boldsymbol{u}}_m(\boldsymbol{x}, t)$ as the response in domain Ω_m, in time $t \in [0, T]$. From now on, this response from the frontal problem will be referred to as *'experimental data'*. The scheme of the domain of interest for the frontal and reverse problem is shown in Figure 2.

2.2.2 Definition of the reverse problem as a source identification problem

The problem of TR is considered as a passive detection of source in Ω_S from the frontal problem in the domain Ω with some information about the response in Ω_m. It is assumed that the region Ω_S is not known and we know the *'experimental data'* $\boldsymbol{u}_m(\boldsymbol{x}, t)$ or $\dot{\boldsymbol{u}}_m(\boldsymbol{x}, t)$ in Ω_m.

First, the "reverse time" τ for the reverse problem has to be defined.

The reverse time τ is defined by transformation in time as $\tau = T - t$. This means that the time τ is going backwards with respect to the time t of the frontal problem. It is also necessary to define the "reversal field variable" – the displacement of the reverse problem $\boldsymbol{w}(\boldsymbol{x}, \tau)$, $\boldsymbol{x} \in \Omega$, $\tau \in [0, T]$. The same geometry and material properties are retained for the inverse problem as for the frontal problem. Also the boundary conditions defined by the operator $\mathbb{B}$ should be the same. Under these conditions, it is possible to satisfy the same wave speeds and boundary conditions for reflection and transmitted wave propagation as for the frontal problem. The boundary and initial conditions for the reversal displacement field $\boldsymbol{w}(\boldsymbol{x}, \tau)$ are obtained from the measurement data $\boldsymbol{u}_\mathrm{m}$ and $\dot{\boldsymbol{u}}_\mathrm{m}$. Furthermore, the time history of the measurement data $\boldsymbol{u}_\mathrm{m}$ and $\dot{\boldsymbol{u}}_\mathrm{m}$ in the domain Ω_m must be taken into account as an extra boundary condition in the domain Ω_m, i.e. $\boldsymbol{w}(\boldsymbol{x}, \tau) = \boldsymbol{u}_\mathrm{m}(\boldsymbol{x}, t)$ and $\dot{\boldsymbol{w}}(\boldsymbol{x}, \tau) = -\dot{\boldsymbol{u}}_\mathrm{m}(\boldsymbol{x}, t)$, $\boldsymbol{x} \in \Omega_\mathrm{m}$. In [49] it is mentioned that the measured velocity $\bar{v}$ should be taken with the opposite sign because of the time derivative with respect to time τ. The proof is found in the definition of the time derivative $\partial/\partial\tau = -\partial/\partial t$, which comes from the definition of the reversal time $\tau = T - t$. In the following text, the bar, $\bar{\square}$, is used to denote the reverse problem quantities.

The reverse problem then takes form

$$\nabla \cdot \bar{\boldsymbol{\sigma}} = \rho \ddot{\boldsymbol{w}}, \quad \bar{\boldsymbol{\sigma}} = \boldsymbol{C} \colon \bar{\boldsymbol{\varepsilon}}, \quad \bar{\boldsymbol{\varepsilon}} = \frac{1}{2}(\nabla \boldsymbol{w} + (\nabla \boldsymbol{w})^\intercal), \quad 0 \leq \tau \leq T, \quad \boldsymbol{x} \in \Omega, \tag{2a}$$

with boundary conditions

$$\mathbb{B}\boldsymbol{w} = \boldsymbol{0} \text{ on } \partial\Omega, \tag{2b}$$

and with initial conditions

$$\boldsymbol{w}(\boldsymbol{x}, 0) = \boldsymbol{0}, \quad \dot{\boldsymbol{w}}(\boldsymbol{x}, 0) = \boldsymbol{0} \quad \boldsymbol{x} \in \Omega, \tag{2c}$$

and with kinematic conditions on Ω_m for TR identification as follows

$$\boldsymbol{w}(\boldsymbol{x}, \tau) = \boldsymbol{u}_\mathrm{m}(\boldsymbol{x}, t), \quad \dot{\boldsymbol{w}}(\boldsymbol{x}, \tau) = -\dot{\boldsymbol{u}}_\mathrm{m}(\boldsymbol{x}, t) \quad \boldsymbol{x} \in \Omega_\mathrm{m}. \tag{2d}$$

For details on the TR problem formulation, see the work of [39]. Prescribing these kinematic conditions $\boldsymbol{w}(\boldsymbol{x}, \tau)$ and $\dot{\boldsymbol{w}}(\boldsymbol{x}, \tau)$ on Ω_m into the governing equations (2) provides the time reversal of the original problem defined in Section 2.2.1.

3 Aim of the thesis

This work aims to improve the reconstruction of the exciting signal in the time domain, meaning some present or forming flaw in the material, and to determine the proper procedure for deployment of TR in practice, i.e., in commercial FE software.

It is intended to achieve the stated aim through the following objectives:

1. *Development of a numerical linear elastodynamic solver suitable for time reversal application*
   Common commercial FE software does not provide full control over analysis settings. For this reason, own linear elastodynamic solver will be developed to control the entire process. It will merge the desired FEM procedures with non-standard time-varying boundary conditions and automate the TR process.

2. *Development of a suitable methodology for FEM based TR (correct reconstruction of the source signal)*
   Several works are dedicated to investigating or improving the quality of the reconstruction of the original source, but a methodology for performing TR in standard and widely used numerical methods such as FEM has not yet been fully established. The most important step in using TR in practice is the correctness of the reconstruction of the original source, and such a methodology will be developed. To evaluate the methodology, several cost functions will be defined.

3. *Sensitivity analysis of computational TR process*
   The effect of changing the input parameters between the direct and inverse tasks, such as temperature, time step size, mesh size, number of signals used, domain shape (domain with a hole), and environmental disturbance (background noise) on the reconstruction of the original pulse will be investigated. In each study, only one parameter will be changed and the result will be compared to the reference one.

4. *Reconstruction of a real source using experimental data*
   The aim of this work is to improve the quality of the reconstruction of the original pulse, and therefore it will culminate in the use of the experimental data. The sensitivity to the number of used loading signals and their position will be further analyzed.

4 Results of the PhD research

4.1 TR-FEM solver

Taking into account the necessity of combining specific procedures to solve the chosen problem, a dynamic solver was developed in MATLAB software. In this work, the solver is called *TR-FEM*. Its capabilities are stated below and the description of the numerical procedures is covered in the theoretical part of the Thesis.

- Linear elastodynamics – 2D + 3D
  – for 2D, plane strain, plane stress, and axial symmetry are possible
- Explicit time integration
  – *leapfrog* form of the central difference method
  – the time integration also includes Δt_{crit} estimations
  – accurate computation according to the formula $\Delta t_{\text{crit}} = \frac{2}{\omega_{\max}}$ is possible
- Full and reduced integration
  – first and second order serendipity quadrilateral and hexagonal elements are implemented
- Hourglass control
  – in the form of an additional stiffness matrix
- Mass matrix lumping
  – row-sum, and HRZ algorithm
- Non-standard time-varying boundary conditions – needed for comparison with the paper in which the inspiration was found
- Rigid body modes filtering
  – for free-floating bodies
- Others: Newmark method, periodic boundary conditions (node2node), contact

4.2 Numerical simulation of the reverse problem

It is assumed that only the normal component of the velocities $\dot{\boldsymbol{u}}_{\mathrm{m}}(\boldsymbol{x},t)$ at the boundary $\partial\Omega_{\mathrm{m}}$ is recorded as the response of the frontal problem. This simulates recording the response in terms of normal velocities at $\partial\Omega_{\mathrm{m}}$ by piezo-sensor or other measurement techniques. Then, $\dot{\boldsymbol{w}}_{\mathrm{m}}(\boldsymbol{x},\tau)$ is computed via (2d). This process is called *time reversal of signal*. In this way the *'experimental data'* for the TR task defined in (2d) are generated by the numerical model. Then, the boundary conditions must be applied in a suitable form to the reverse problem. For the application of the boundary conditions in Ω_{m} in the FE simulation, two forms are considered, only on $\partial\Omega_{\mathrm{m}}$, as

Type I: loading by normal velocity components in the Dirichlet sense

$$\dot{\boldsymbol{w}}^{\mathrm{n}}_{\mathrm{m}}(\boldsymbol{x},\tau) \quad \boldsymbol{x}\in\partial\Omega_{\mathrm{m}}, \quad 0\le\tau\le T, \tag{3a}$$

Type II: loading by normal stress components in the Neumann sense

$$\boldsymbol{\sigma}^{\mathrm{n}}_{\mathrm{m}}(\boldsymbol{x},\tau)=\sigma^{\mathrm{n}}_{\mathrm{m}}(\boldsymbol{x},\tau)\boldsymbol{n}=A\dot{\boldsymbol{w}}^{\mathrm{n}}_{\mathrm{m}}(\boldsymbol{x},\tau) \quad \boldsymbol{x}\in\partial\Omega_{\mathrm{m}}, \quad 0\le\tau\le T. \tag{3b}$$

Here, $\boldsymbol{n}$ is the outward normal direction to the boundary $\partial\Omega_{\mathrm{m}}$. A is a constant with a suitable value depending on the material parameters. For this normal traction loading $\boldsymbol{\sigma}_{\mathrm{n}}$ the external nodal force vector is generated as $\boldsymbol{f}_{\mathrm{ext}}$. This process can be viewed as a transfer of the Dirichlet boundary conditions of velocity $\dot{\boldsymbol{w}}^{\mathrm{n}}_{\mathrm{m}}$ meaning to Neumann boundary condition as normal stress $\boldsymbol{\sigma}^{\mathrm{n}}_{\mathrm{m}}$ in $\partial\Omega_{\mathrm{m}}$.

4.2.1 Loading and boundary conditions

To solve the system $\mathbf{M}\ddot{\mathbf{u}}(t)+\mathbf{K}\mathbf{u}(t)=\mathbf{f}(t)$, the suitable Dirichlet and Neumann boundary and initial conditions for frontal and reverse problems should be included. In the finite element method, the kinematic boundary conditions can be prescribed by given nodal displacements, velocities or accelerations, for details see [51] or [52].

In the following algorithm, (4a)–(4e), the prescribed quantities in CD schemes are meant to be prescribed only at some nodes. This effect is not additionally emphasized in the symbols used for better readability. Also, the asterisk in the lower index, $\square_*$, denotes the prescribed value in the corresponding time, and the symbol := denotes the assignment of the prescribed value.

Application of 'loading' Type I - red color

The CD scheme was modified in order to include the measurement data in the form of normal velocities $\dot{\mathbf{w}}_{\text{normal}}$ as Type I. In the following algorithm the desired values of velocity, marked in red, at the boundary $\partial\Omega_{\text{m}}$ are prescribed as $\dot{\mathbf{u}}_*$.

Application of 'loading' Type II - blue color

In Type II, loading in the form of a prescribed external nodal force $\mathbf{f}_{\text{ext},*}$, marked in blue, is assumed at $\partial\Omega_{\text{m}}$ due to a normal traction loading with the given time history.

$$\dot{\mathbf{u}}\left(t+\tfrac{\Delta t}{2}\right) = \dot{\mathbf{u}}(t) + \ddot{\mathbf{u}}(t)\tfrac{\Delta t}{2} \tag{4a}$$

apply prescribed nodal velocity as

$\dot{\mathbf{u}}(t+\frac{\Delta t}{2}) := \dot{\mathbf{u}}_*(t+\frac{\Delta t}{2})$ at $\partial\Omega_{\text{m}}$

$$\mathbf{u}(t+\Delta t) = \mathbf{u}(t) + \dot{\mathbf{u}}\left(t+\tfrac{\Delta t}{2}\right)\Delta t \tag{4b}$$

apply prescribed nodal force as

$\mathbf{f}_{\text{ext}}(t+\Delta t) := \mathbf{f}_{\text{ext}}(t+\Delta t) + \mathbf{f}_{\text{ext},*}(t+\Delta t)$ at $\partial\Omega_{\text{m}}$

$$\mathbf{r}(t+\Delta t) = \mathbf{f}_{\text{ext}}(t+\Delta t) - \mathbf{K}\mathbf{u}(t+\Delta t) \tag{4c}$$

$$\ddot{\mathbf{u}}(t+\Delta t) = \mathbf{M}^{-1}\mathbf{r}(t+\Delta t) \tag{4d}$$

$$\dot{\mathbf{u}}(t+\Delta t) = \dot{\mathbf{u}}\left(t+\tfrac{\Delta t}{2}\right) + \ddot{\mathbf{u}}(t+\Delta t)\tfrac{\Delta t}{2} \tag{4e}$$

apply prescribed nodal velocity as

$\dot{\mathbf{u}}(t+\Delta t) := \dot{\mathbf{u}}_*(t+\Delta t)$ at $\partial\Omega_{\text{m}}$

Remark: If the prescribed velocity is updated with the desired value as in [39], i.e. $\dot{\mathbf{u}}^t := \dot{\mathbf{u}}^t + \dot{\mathbf{u}}_*^t$, with a scaling parameter $\mathcal{C}$, while the choice of $\mathcal{C}$ is subjected to preservation of the linear momentum balance, then for one node as a mass point with the mass m the relation obtained is

$$\dot{\mathbf{u}}^{t+\frac{\Delta t}{2}} := \dot{\mathbf{u}}^t + \mathcal{C}\cdot\dot{\mathbf{u}}_*^{t+\frac{\Delta t}{2}}. \tag{5}$$

Then the impulse-momentum theorem is used

$$\mathbf{I}_{\text{f}} = \int_t^{t+\Delta t} \mathbf{f}_*(t)\mathrm{d}t = \mathbf{p}(t+\Delta t) - \mathbf{p}(t) = \Delta\mathbf{p} = m\Delta\dot{\mathbf{u}} \tag{6}$$

where $\mathbf{I}_{\text{f}}$ is the impulse of the force and $\mathbf{p}$ is the linear momentum defined as $\mathbf{p} = m\dot{\mathbf{u}}$. Respecting using half-steps for prescription of the

velocity, the relation derived is

$$\frac{\Delta t}{2}\mathbf{f}_* \equiv m \cdot \Delta\dot{\mathbf{u}}_{*\,\frac{\Delta t}{2}}, \tag{7}$$

where m is nodal mass, $\Delta\dot{\mathbf{u}}_{*\,\frac{\Delta t}{2}}$ is the change of the nodal velocity between times t and $t + \frac{\Delta t}{2}$ from the equation (5), and f_* is the acting equivalent nodal force. Hence, coefficient $\mathcal{C} = \frac{2 \cdot m}{\Delta t}$. It is apparent that with this way of prescription of the nodal velocity with updating $\dot{\mathbf{u}}^t := \dot{\mathbf{u}}^t + \mathcal{C}\dot{\mathbf{u}}^t_*$ the same result is obtained, with numerical accuracy, as with the loading by the corresponding nodal force $\mathbf{f}_*$ and no further scaling of the recorded signals is necessary.

4.2.2 Problem definition

For all the following numerical experiments in this section (Section 4.2), a two-dimensional square domain under plane stress condition with stress-free boundary is considered, see its dimensions in Figure 3a [1]. In this figure, the $\boldsymbol{\mathcal{A}}$ and $\boldsymbol{\mathcal{B}}$ regions mark the position of application of the original source and the position where the response is recorded, respectively. The locations of these regions were chosen arbitrarily, but $\boldsymbol{\mathcal{B}}$ should belong to the boundary. In $\boldsymbol{\mathcal{A}}$, 3×3 nodes are prescribed the loading, while in $\boldsymbol{\mathcal{B}}$, the number of nodes varies and is specified in each task description. The length of the element edge is 0.4 mm, thus the FE mesh consists of 62,500 bilinear four-noded elements. The mesh was defined with respect to the maximum frequency contained in the loading signal and the dispersion behavior of the finite element method, see [53, 54], or [4, 7, 8].

A linear homogeneous isotropic material is assumed with Young's modulus $E = 2 \cdot 10^{11}$ Pa, Poisson's ratio $\nu = 0.3$, and mass density $\rho = 7,850$ kg·m^{-3}, with neither material nor numerical damping. The longitudinal wave speed for plane stress problem is given as $c_{\text{L}} = \sqrt{\frac{E}{(1-\nu^2)\rho}} \doteq 5,291.3$ m·s^{-1}. Time step size Δt is set to $4.009 \cdot 10^{-8}$ s resulting in the Courant number $Co \doteq 0.75$.

For loading function $\boldsymbol{f}_{\text{ext}}(t) = A_0 R(t)$ in the region $\boldsymbol{\mathcal{A}}$, where A_0 is the amplitude of loading, the Ricker pulse is used, [55], which is given by a parametric formula with parameter p as

$$R(p) = -\frac{\sqrt{2\pi} \cdot \sigma \cdot \left(\left(\frac{p}{\sigma}\right)^2 - 1\right) \cdot e^{\left(-0.5 \cdot \left(\frac{p}{\sigma}\right)^2\right)}}{\sqrt{2\pi} \cdot \sigma}, \tag{8}$$

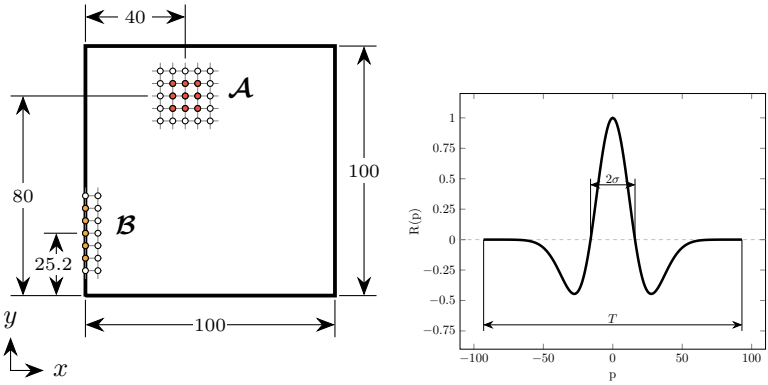

(a) *Scheme of the domain of interest, [mm] [1].* **(b)** *Loading Ricker pulse with its parameters [1].*

Figure 3: *Problem definition for reconstruction test.*

where $\sigma = 16 \cdot \Delta t$ and $p = \langle -93, 93 \rangle \cdot \Delta t$, the transformation between parameter p and time t is $t = p + 93 \cdot \Delta t$, and T is then 7.49683^{-6} s, see Figure 3b. Amplitude $A_0 = 1$ in all numerical experiments.

The Ricker pulse was chosen for the reason that this pulse is symmetrical and also the areas above and below the horizontal zero line are the same. This means that the total impulse of the pulse is equal to zero. This implies that loading with a Ricker pulse does not accelerate a free body and all kinematic quantities have a meaningful value.

4.2.3 Reconstruction test and proposed methodology

This test is performed to analyze the effect of different types of boundary conditions on the accuracy of the reconstruction of the original source. With these findings, it was possible to propose a flowchart for the implementation of the appropriate scheme with the application of TR boundary conditions for accurate reconstruction in TR tasks.

Numerical response to loading TYPE II in frontal task

First, the response to nodal force loading (TYPE II) in the frontal task was investigated to gain a better understanding of an optimal application of boundary conditions in the TR problem. The nodal force loading is applied to nodes in the region $\mathcal{A}$ in the y-direction

with the time function of the Ricker pulse. The kinematic quantities, namely the y-component of displacement, velocity and acceleration in the central node of $\boldsymbol{\mathcal{A}}$ are recorded, see Figure 4 [1]. The result shows that the time history of the displacement in $\boldsymbol{\mathcal{A}}$ corresponds to the time function of the loading nodal force. This means that the time function of the nodal force loading must be an integral of the desired nodal velocity in order to force the desired motion in terms of velocity. The following numerical test shows the verification of this idea for a correct time reversal.

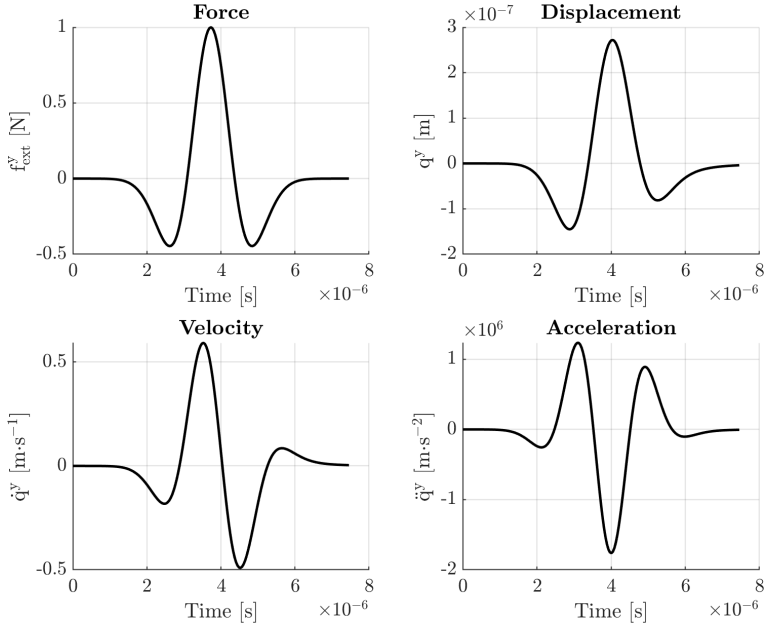

Figure 4: *Output quantities in the y-direction at the middle point of loading by nodal force. The time function of nodal force (top-left) was applied as a load [1].*

Numerical verification of proposed procedure

Now, a sequence of time integration of the original loading pulse (the Ricker pulse) and time integration of a velocity signal recorded in the region $\boldsymbol{\mathcal{A}}$ is examined.

The computations are marked as **Int** − **Int**, **Int** − **Orig**, **Orig** − **Int**, and **Orig** − **Orig**, where the first key means the loading time function in the region $\mathcal{A}$ for the forward task, and the second key means the loading time function in the region $\mathcal{B}$ for the reverse task after reversing the responding signal in time. The key **Int** denotes the time integration of the pulse and **Orig** denotes the pulse without modification, i.e., without time integration. For example, the combination **Int** − **Orig** means, that the time function in the region $\mathcal{A}$ is integrated in time and the time function recorded in the region $\mathcal{B}$ is not integrated with respect to time and only reversed in time. Then it is applied as loading into the reverse task. For the numerical time integration of the signal, the trapezoidal rule is employed with the time step size as for the FE computation. Four combinations of keys occur (**Int** − **Int**, **Int** − **Orig**, **Orig** − **Int**, **Orig** − **Orig**) and this results in four reconstructed signals.

In general, the amplitudes of loading in the regions $\mathcal{A}$ and $\mathcal{B}$ must be chosen with respect to the accuracy of computation, the scale of the problem, and the material properties of the domain of interest.

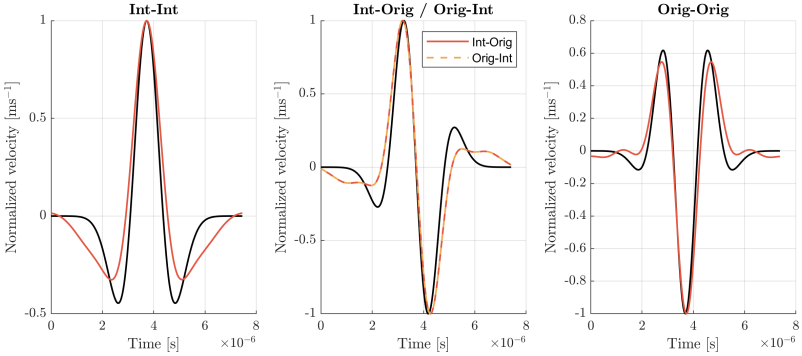

Figure 5: *Reconstructions of the original source for four different combinations of modification of loading signals in frontal and reverse problems, denoted as* **Int** *and* **Orig**. *The first indication refers to frontal problem, the second one refers to reverse problem. The keys* **Int** *marks the time integration of the pulse and* **Orig** *marks the pulse without modification, i.e. without time integration [1].*

The results normalized with respect to the maximum value are shown in Figure 5 (red/orange lines) [1]. These plots summarize the time histories of the y-component of the reconstructed velocity in the region $\boldsymbol{\mathcal{A}}$ are summarized for all combinations of both integrated and non-integrated loading signals after the entire TR process. It is needed to say that with respect to the linearity of the problem, combinations **Int** − **Orig**, **Orig** − **Int** produce the same results. In all sub-figures the corresponding (analytically calculated) time derivative of the loading pulse is plotted as a black line.

In the left sub-figure, the black line corresponds to the Ricker pulse as an original loading pulse, in the middle sub-figure, the black line corresponds to the first time derivative, and finally, in the right sub-figure, the black line corresponds to the second time derivative. It is clear, that the combination **Int** − **Int** produces the correct time history of the original pulse of the nodal velocity. The combination **Int** − **Orig**/ **Orig** − **Int** gives the first time derivative of the original pulse, and the combination **Orig** − **Orig** gives the second time derivative of the original pulse. This means, metaphorically, that during the numerical TR process (forward and reverse tasks together) two time derivatives of the original pulse are lost - each computation changes the time derivative of the output signal with respect to the input signal. This phenomenon can be explained by the impulse-momentum theorem (6), where there is a relation between the time history of the applied force and the derived velocity.

Based on the previous results, for the correct reconstruction of the original pulse, one need to precede the time integration of the loading pulse both before frontal and reverse task of the TR process. With this knowledge the algorithm for computational TR is proposed, Alg. 1. This algorithm, if all steps are followed, leads to a "topologically" correct reconstruction of the original source. On the left side of the algorithm one can see the flowchart for the full computational approach for TR computations with the generation of the *'experimental data'* on the domain Ω_{m} numerically. On the right side one can see the flowchart for the application of TR with real experimental data in terms of measured velocities.

FRONTAL PROBLEM

COMPUTATION

1. **INTEGRATE LOADING SIGNAL OF DESIRED VELOCITY**
   Integrate the loading signal e.g. by trapezoidal rule.

2. **PRESCRIBE LOADING AS NODAL FORCE**
   Obtained time history of nodal velocity corresponds to the first derivative of time history of nodal force loading.

3. **PERFORM COMPUTATION**
   Output from frontal problem is a time history of nodal velocity from measurement area.

OR

EXPERIMENT

1. **GET MEAUSERD SIGNAL**
   Get measured signal of velocity from measurement area. This signal can be edited using standard procedures by e.g. frequency filter.

REVERSE PROBLEM

BOTH FROM COMPUTATION OR EXPERIMENT

4. **MULTIPLY OUTPUT SIGNAL BY -1**
   Multiply the output signal of velocity by -1. This operation is given by TR principle, see e.g. [39].

5. **INTEGRATE SIGNAL**
   Integrate time history of velocity, same as in step 1.

6. **REVERSE SIGNAL IN TIME**
   Reverse the output signal to create a loading signal.

7. **USE SIGNAL AS LOADING BY NODAL FORCE**
   Same as in step 2, obtained time history of nodal velocity corresponds to the first derivative of time history of nodal force loading.

8. **PERFORM COMPUTATION**
   Compute the reverse problem.

9. **REVERSE OUTPUT SIGNAL IN TIME**
   Take time history of nodal velocity from the original source location and reverse it in time to compare with the loading pulse (of desired nodal velocity).

Algorithm 1: *Proposed algorithm for practical use of time reversal method. On the left is the computational/computational approach, and on the right is the experimental/computational approach.*

4.2.4 Key verification of the proposed methodology

In this series of numerical experiments, two types of loading for application in TR tasks are compared – TYPE I (nodal velocity) and TYPE II (nodal force). This compares two approaches how to solve the problem with standard methods in commercial FE software. The effect of the size of the domain Ω_{m} on the quality of the reconstruction is also examined in a form of different numbers of active nodes in the reverse task, to which the nodal information is prescribed. Five different numbers of loaded nodes are assumed – one node, five nodes and eleven nodes with separate signals, and the same numbers with averaged signals. The computations were performed for time $T = 0.00400900$ s, which corresponds to approximately 212 reflections of the longitudinal wave between opposite edges.

The time histories of the normalized velocity after TR computation of the both types of loading are shown in Figure 6 [1] (loading by nodal velocity) and Figure 7 [1] (loading by nodal force). Each reconstructed signal is normalized so that the maximum value is equal to 1, assuming a linear system that can be scaled arbitrarily. Then the signals are reversed in time, although this is not necessary due to the symmetry of the loading signal. This normalization of the signals allows at least some qualitative comparison of the reconstruction.

There is also an influence of the number of active nodes on the quality of the reconstruction. From the physical point of view, when the prescribed signal is applied as the nodal velocity, the boundary is moved in a rigid way and this boundary reflects the propagating waves as rigid boundary, which has opposite an effect on the reflection of stresses than the stress-free boundary conditions, see e.g. the book of Achenbach on wave propagation in solids, [56]. Therefore, the TYPE II leads to more stable results of the reconstruction, see Figure 7 [1]. With larger number of active nodes for the application of boundary conditions, this effect is even amplified.

For the loading TYPE I, one can see a different arrival time of the maximum peak, depending on the number of active nodes in the reverse task and averaging of the reversed quantities. On the contrary, the results for the loading TYPE II show a stable character and deviation of the signal is relatively small. This means that the loading TYPE II is preferred for a correct reconstruction of the original signal.

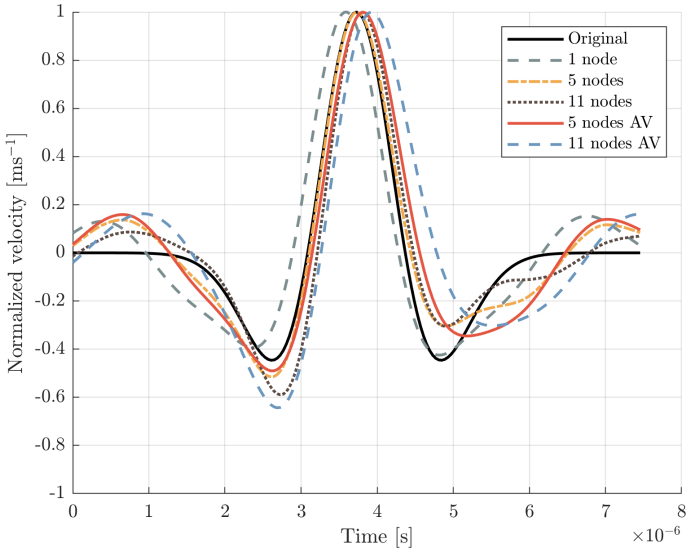

Figure 6: *Reconstructed pulse for loading TYPE I [1].*

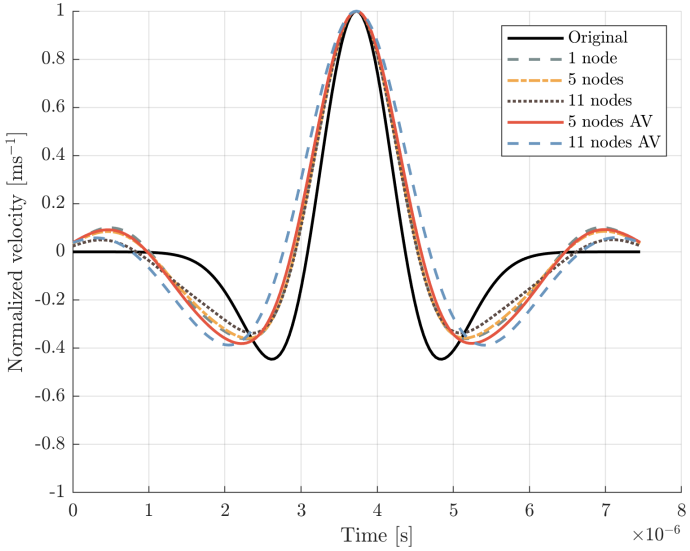

Figure 7: *Reconstructed pulse for loading TYPE II [1].*

4.3 TR with experimental data

This section presents the not yet published results of using real experimental data to reconstruct the original source in the time domain using the proposed methodology. The paper is in preparation.

In this section, the experimental data from the paper [2] were used for reconstruction of the original source. In the mentioned paper, we worked only with three measured signals at points A, B, and C, but in fact 195 signals were recorded. These responding signals were used for the reconstruction of the original loading signal. In accordance with the proposed procedure, see Algorithm 1, the recorded signals of normal velocity were time-reversed and integrated and used as a pressure load in the reverse task.

A thin aluminum plate was loaded by a piezoelectric transducer at the center of the bottom edge. The dimensions of the plate were 399 × 50 × 1.35 mm and the material properties were $E = 72$ GPa, $\nu = 0.333$, $\rho = 2770$ kg·m^{-3}. The FE mesh consisted of 1596 × 200 = 319200 4-noded quadrilateral elements, the length of the element edge was 0.25 mm, Δt was 4.5 ·10^{-8} s. The response in terms of normal velocity was recorded at the top edge in 195 points with a spatial step of 1 mm, symmetrically distributed with respect to the central point, which was exactly opposite to the transducer. See the scheme in Figure 8.

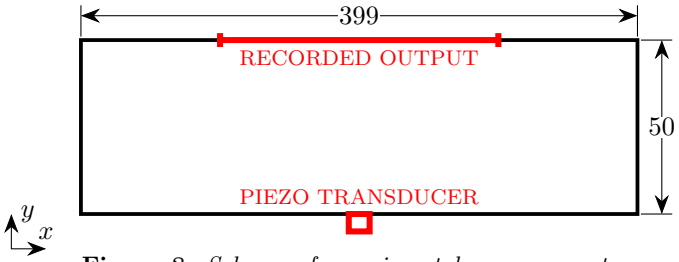

Figure 8: *Scheme of experimental measurement.*

The loading corresponded to a smooth pulse of duration t_0 with amplitude σ_0 changing according to a cosine train 333 kHz with 0.25 cosine window, sampled at 20 MHz. The shape of the loading is given in Figure 9. The response was recorded one after another in all 195 points with the vibrometer. For a more detailed description of the experimental setup, see [2]. See the x-t plot of the recorded normal velocity for the first 1000 time steps in Figure 10.

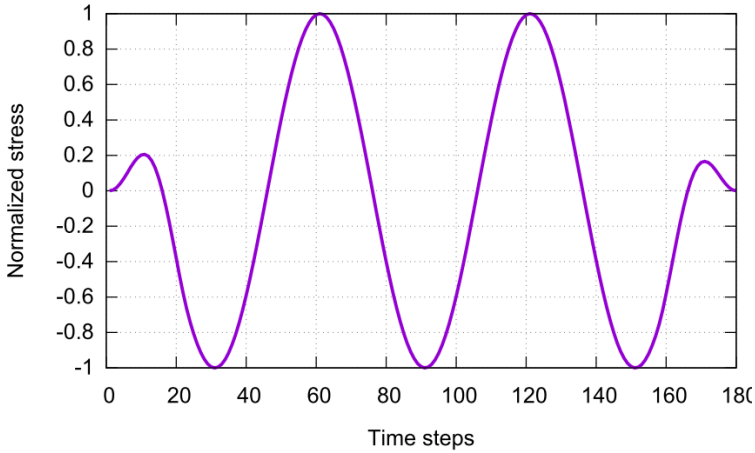

Figure 9: *Loading signal.*

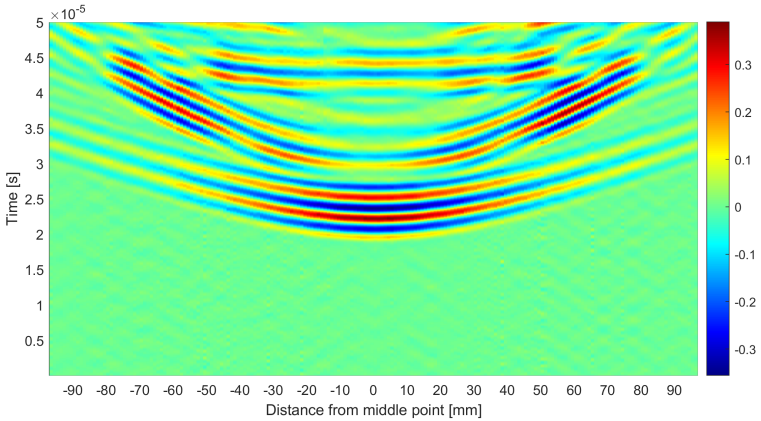

Figure 10: *X-t plot of measured normal velocities.*

Unlike purely numerical experiments, such as in Section 4.2, where the time history of the velocity in the loaded area is known and the reconstruction can be directly compared and assessed using, e.g., the proposed cost functions, in a real experiment the velocity excited by the transducer cannot be recorded, so the reference signal does not exist. Therefore, the real velocity pulse recorded at the center of the

transducer was used as the reference signal for comparison with the reconstruction. Because of the uncertainties with exact start of the loading and with the exact shape of the loading signal, it was not straightforward how to assess the quality of the reconstruction, and the result is assessed only visually.

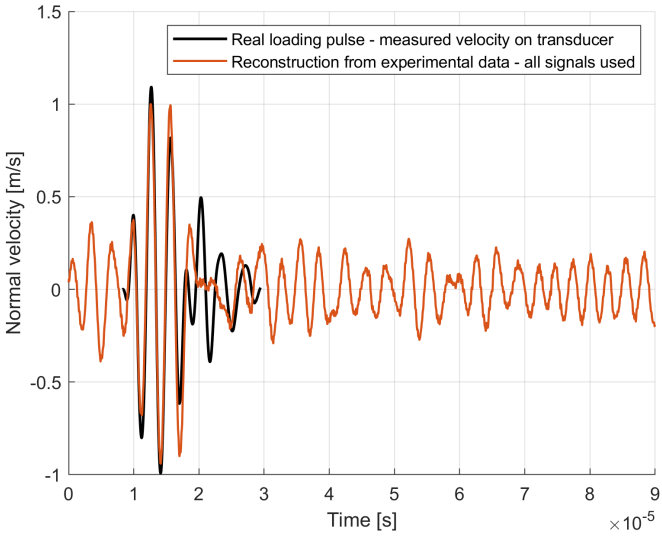

Figure 11: *Result of TR.*

The reconstructed signal in Figure 11 was "positioned" to match the reference signal by shifting it in both the x and y directions. The criterion for the y-shift was purely visual and the criterion for the x-shift (time) was the value of the cross-correlation of both signals. The magnitude of the reconstructed signal was also arbitrarily updated. The positioning of the reconstructed signal is possible due to the linearity of the problem. The same post-processing of the reconstruction will be necessary in any kind of real employment of TR for the lack of knowledge of the source signal. The results prove that the proposed methodology works well and provides a correct reconstruction of the source in the time domain.

5 Discussion

In this thesis, the use of the computational time reversal method for reconstruction of the original source was investigated. In order to be able to analyze such a problem and have a full control over the analysis, an **explicit solver called *TR-FEM*** was developed. *TR-FEM* combines the desired numerical procedures with non-standard time-varying boundary conditions and automates the TR process.

The numerical solution of direct wave propagation in a homogeneous body was tested and compared with the experiment and the analytical solution, which, among other things, served as a **verification of the code**. Up to a certain time, a good agreement of all methods was achieved. Similarly, the solutions with the analytical approach, the finite element method, and the finite volume method of direct wave propagation in a heterogeneous body were compared.

Afterwards, a detailed analysis of prescribing various time-varying boundary conditions was performed. First, the initial wave field was reconstructed, then a loading pulse was used. Based on this analysis was **developed a procedure** of how to prescribe loading signal to keep the correct time history of all kinematic quantities. For evaluation of quality of the original source reconstruction the proposed cost functions were used.

For verification of the developed methodology, the real experimental data were used in a numerical model for **reconstruction of the real source**. The model was loaded with recorded signals from different positions and the reconstructions were compared. The developed methodology **proved to be successful** and thus allows the original source to be reconstructed in the time domain.

Further, other numerical tests were carried on to show what are the possibilities and limitations of the method. Namely influence of change of temperature on quality of reconstruction, localization of source using cross-correlation of two recorded signals, and localization of emerging and propagating crack modeled by disconnected nodes.

This work adds another piece to the puzzle called the digital twin. The whole concept of the digital twin can only be fully effective if it provides complete information and the nature of the excitation source is as important as its localization.

As the analysis of the influence of temperature implies, the quality of the reconstruction is **highly sensitive** to the input parameters. The success of using this method depends on the precise tuning of the ma-

terial properties of the tested body. In practice, it would be necessary to first calibrate the model and transfer the material properties from the real to the digital model with sufficient accuracy.

Recommendations for future research

In order to identify the type of flaw such as an emerging crack, an impact, or a loose screw connection, it is necessary to know how such a flaw behaves. In other words, what the derived source signal looks like. As part of further research, it would be useful to create a database of these signals in order to be able to evaluate the types of flaws. Needless to say, the explicit computation is highly time demanding. By definition, the time reversal method works with local sources and such sources are linked with higher frequencies. Future research could investigate applying some model order reduction procedure.

6 Conclusions

This research was conducted to improve the quality of the reconstruction of the original source using the computatinal time reversal method. A procedure for correctly prescribing the loading signal was developed and verified on experimental data, and several numerical tests were performed as a benchmark. **The objectives of the dissertation were met.** It can be concluded that with a sufficient amount of information loaded (temporal and spatial) it is possible to reconstruct the original source in the time domain correctly. Therefore, the use of the computational time reversal method in practice is feasable if the parameters of the computational model are sufficiently calibrated.

References

Author's peer-reviewed journal papers

[1] M. Mračko, J. Kober, R. Kolman, Z. Převorovský, A. Tkachuk, and J. Plešek. "Finite Element Method Based Computational Time Reversal in Elastodynamics: Refocusing, Reconstruction and Its Numerical Sensitivity". In: *Mathematics and Computers in Simulation* 189 (Nov. 2021), pp. 163–190.

[2] M. Mračko, V. Adámek, A. Berezovski, J. Kober, and R. Kolman. "Experimental, Analytical, and Numerical Study of Transient Elastic Waves from a Localized Source in an Aluminium Strip". In: *Applied Acoustics* 178 (July 2021), p. 107983.

[3] V. Adámek, A. Berezovski, M. Mračko, and R. Kolman. "A Two-Layer Elastic Strip under Transverse Impact Loading: Analytical Solution, Finite Element, and Finite Volume Simulations". In: *Mathematics and Computers in Simulation* 189 (Nov. 2021), pp. 126–140.

Author's conference journal papers

[4] A. Kruisová, R. Kolman, M. Mračko and M. Okrouhlík. "Temporal-Spatial Dispersion Analysis of Finite Element Method in Implicit Time Integration". In: *Engineering mechanics - Book of full texts* (2019).

[5] D. Gabriel, A. Tkachuk, J. Kopačka, R. Kolman, M. Mračko, M. Bischoff and J. Plešek. "Estimation of Stability Limit Based on Gershgorin's Theorem for Explicit Contact-Impact Analysis Signorini Problem Using Bipenalty Approach". In: *6th International conference on computational methods in structural dynamics and earthquake engineering - Proceedings* (2017).

Author's technical reports

[6] D. Mochar, M. Mračko, D. Gabriel, R. Kolman and J. Kopačka. *Metodika pro Modelování Dynamických Deju Metodou Konecných Prvku - Fáze II.* Technical report. Institute of thermomechanics of the CAS, v. v. i.: Česká zbrojovka a.s., 2017.

Author's conference talks

[7] A. Kruisová, R. Kolman and M. Mračko. "Full Dispersion Analysis of the Newmark Family in Finite Element Method in Elastodynamics". In: Computational Mechanics. Vol. 2017. Špičák.

[8] A. Kruisová, R. Kolman and M. Mračko. "Dispersion Errors for Wave Propagation in Thin Plate Due to the Finite Element Method". In: Computational Mechanics. Vol. 2019.

[9] J. Kober, M. Mračko and Z. Převorovský. "Verification of Digital Twin Concept for Time Reversal Analysis". In: NDT in Progress. Vol. 2019. Praha.

[10] M. Mračko, A. Tkachuk, R. Kolman, J. Plešek and D. Gabriel. "Comparison of Local and Global Critical Time Step Size Estimators in Explicit Dynamics". In: Computational Mechanics. Vol. 2016. Špičák.

[11] M. Mračko, R. Kolman, A. Tkachuk, J. Kopačka, D. Gabriel and J. Plešek. "Comparison of Local and Global Critical Time Step Size Estimators in Explicit Dynamics: Multidimensional Case". In: ECCOMAS Young Investigators Conference. Vol. 2017. Milano.

[12] M. Mračko, A. Tkachuk, R. Kolman, J. Plešek and D. Gabriel. "Critical Time Step Estimators in Explicit Dynamics". In: Computational Mechanics. Vol. 2017. Špičák.

[13] M. Mračko, J. Kober, R. Kolman, Z. Převorovský, J. Plešek, J. Masák and A. Kruisová. "On Finite Element Modelling in Time Reversal Problem". In: IX Th NDT in Progress. Vol. 2017. Praha.

[14] M. Mračko, R. Kolman, J. Kober, Z. Převorovský and J. Plešek. "Influence of Temperature in Computational Time Reversal Method". In: The 2nd International Conference on Advanced Modelling of Wave Propagation in Solids. Vol. 2018. Praha.

[15] M. Mračko, R. Kolman, J. Kober, Z. Převorovský and J. Plešek. "Computational Time Reversal Method Based on Finite Element Method: Influence of Temperature". In: Engineering Mechanics. Vol. 2018. Svratka.

[16] M. Mračko, R. Kolman, J. Kober, Z. Převorovský and J. Plešek. "Crack Localization Using Computational Time Reversal Method". In: ECCOMAS Young Investigators Conference. Vol. 2019. Krakow.

[17] M. Mračko, R. Kolman, J. Kober, Z. Převorovský and J. Plešek. “The 2nd International Conference on Advanced Modelling of Wave Propagation in Solids”. In: NDT in Progress. Vol. 2019. Praha.

[18] Z. Převorovský, M. Mračko, J. Kober, J. Krofta and R. Kolman. “Acoustic Source Location by Time Reversal Signal Transfer from Experiment to Numerical Model (Digital Twin)”. In: Advanced Modelling of Wave Propagation in Solids. Vol. 2018. Praha.

[19] Z. Převorovský, J. Krofta, J. Kober, M. Chlada and M. Mračko. “Time Reversal Localization of Continuous and Burst Acoustic Emission Sources under Noise”. In: European Conference on Acoustic Emission Testing. Vol. 2018. Senlis.

Author’s conference posters

[20] M. Mračko, J. Kopačka, A. Tkachuk, R. Kolman, J. Plešek and D. Gabriel. “Application of Gershgorin’s Theorem for Time Step Size Estimation for Contact-Impact Problems”. In: Seminar on Numerical Analysis. Vol. 2017. Ostrava.

Other references

[21] H. Lasi, P. Fettke, H.-G. Kemper, T. Feld, and M. Hoffmann. “Industry 4.0”. In: *Business & Information Systems Engineering* 6.4 (Aug. 2014), pp. 239–242.

[22] H. Cañas, J. Mula, M. Díaz-Madroñero, and F. Campuzano-Bolarín. “Implementing Industry 4.0 Principles”. In: *Computers & Industrial Engineering* 158 (Aug. 2021), p. 107379.

[23] D. Balageas, C.-P. Fritzen, and A. G??emes. *Structural Health Monitoring*. 2010.

[24] A. Ghosh, D. J. Edwards, M. R. Hosseini, R. Al-Ameri, J. Abawajy, and W. D. Thwala. “Real-Time Structural Health Monitoring for Concrete Beams: A Cost-Effective ‘Industry 4.0’ Solution Using Piezo Sensors”. In: *International Journal of Building Pathology and Adaptation* 39.2 (May 11, 2020), pp. 283–311.

[25] D. Goyal, S. Balamurugan, K. Senthilnathan, I. Annapoorani and M. Israr, eds. *Cyber-Physical Systems and Industry 4.0: Practical Applications and Security Management*. First edition. Pam Bay, FL: Apple Academic Press, Inc, 2022. 1 p.

[26] L. F. C. S. Durão, S. Haag, R. Anderl, K. Schützer, and E. Zancul. "Digital Twin Requirements in the Context of Industry 4.0". In: *Product Lifecycle Management to Support Industry 4.0*. Ed. by P. Chiabert, A. Bouras, F. Noël, and J. Ríos. Vol. 540. IFIP Advances in Information and Communication Technology. Cham: Springer International Publishing, 2018, pp. 204–214.

[27] F. Pires, A. Cachada, J. Barbosa, A. P. Moreira and P. Leitao. "Digital Twin in Industry 4.0: Technologies, Applications and Challenges". In: *2019 IEEE 17th International Conference on Industrial Informatics (INDIN)*. 2019 IEEE 17th International Conference on Industrial Informatics (INDIN). Helsinki, Finland: IEEE, July 2019, pp. 721–726.

[28] Y.-C. Choi, J.-H. Park, and K.-S. Choi. "An Impact Source Localization Technique for a Nuclear Power Plant by Using Sensors of Different Types". In: *ISA Transactions* 50.1 (Jan. 2011), pp. 111–118.

[29] H. Yu, L. Lu, and P. Qiao. "Localization and Size Quantification of Surface Crack of Concrete Based on Rayleigh Wave Attenuation Model". In: *Construction and Building Materials* 280 (Apr. 2021), p. 122437.

[30] K. Hensberry, N. Kovvali, K. C. Liu, A. Chattopadhyay and A. Papandreou-Suppappola. "Guided Wave Based Fatigue Crack Detection and Localization in Aluminum Aerospace Structures". In: *Volume 1: Development and Characterization of Multifunctional Materials; Modeling, Simulation and Control of Adaptive Systems; Structural Health Monitoring*. ASME 2012 Conference on Smart Materials, Adaptive Structures and Intelligent Systems. Stone Mountain, Georgia, USA: American Society of Mechanical Engineers, 19th Sept. 2012, pp. 907–916.

[31] J. A. Scales and A. Gersztenkorn. "Robust Methods in Inverse Theory". In: *Inverse Problems* 4.4 (1st Oct. 1988), pp. 1071–1091.

[32] R. S. MacKay and J. D. Meiss, eds. *Hamiltonian Dynamical Systems: A Reprint Selection*. Boca Raton: CRC Press, 2020.

[33] G. Zhang, J. M. Hovem, H. Dong, and L. Liu. "Coherent Underwater Communication Using Passive Time Reversal over Multipath Channels". In: *Applied Acoustics* 72.7 (June 2011), pp. 412–419.

[34] C. He, Q. Zhang, and J. Huang. “Passive Time Reversal Communication with Cyclic Shift Keying over Underwater Acoustic Channels”. In: *Applied Acoustics* 96 (Sept. 2015), pp. 132–138.

[35] S. Dos Santos and Z. Prevorovsky. “Imaging of Human Tooth Using Ultrasound Based Chirp-Coded Nonlinear Time Reversal Acoustics”. In: *Ultrasonics* 51.6 (Aug. 2011), pp. 667–674.

[36] M. Fink, G. Montaldo, and M. Tanter. “Time-Reversal Acoustics in Biomedical Engineering”. In: *Annual Review of Biomedical Engineering* 5.1 (Aug. 2003), pp. 465–497.

[37] M. Fink. “Time Reversal and Phase Conjugation with Acoustic Waves: Industrial and Medical Applications”. In: *Conference on Lasers and Electro-Optics* 3 (2005), pp. 2334–2335.

[38] C. S. Larmat, R. A. Guyer, and P. A. Johnson. “Time-Reversal Methods in Geophysics”. In: *Physics Today* 63.8 (Aug. 2010), pp. 31–35.

[39] D. Givoli and E. Turkel. “Time Reversal with Partial Information for Wave Refocusing and Scatterer Identification”. In: *Computer Methods in Applied Mechanics and Engineering* 213–216 (Mar. 2012), pp. 223–242.

[40] I. Levi, E. Turkel, and D. Givoli. “Time Reversal for Elastic Wave Refocusing and Scatterer Location Recovery”. In: *Journal of Computational Acoustics* 23.01 (Mar. 2015), p. 1450013.

[41] E. Amitt, D. Givoli, and E. Turkel. “Combined Arrival-Time Imaging and Time Reversal for Scatterer Identification”. In: *Computer Methods in Applied Mechanics and Engineering* 313 (Jan. 2017), pp. 279–302.

[42] C. G. Panagiotopoulos, Y. Petromichelakis and C. Tsogka. “Time Reversal and Imaging for Structures”. In: *Lecture Notes in Civil Engineering* 2 (2017), pp. 159–182.

[43] K. Kimoto, K. Nakahata, and T. Saitoh. “An Elastodynamic Computational Time-Reversal Method for Shape Reconstruction of Traction-Free Scatterers”. In: *Wave Motion* 72 (July 2017), pp. 23–40.

[44] Y. Kwak, S. M. Park, J. Lee and J. Park. “Rattle Noise Source Localization through the Time Reversal of Dispersive Vibration Signals on a Road Vehicle”. In: *Wave Motion. An International Journal Reporting Research on Wave Phenomena* 93 (2020), p. 102452.

[45] H. W. Park, S. B. Kim, and H. Sohn. “Understanding a Time Reversal Process in Lamb Wave Propagation”. In: *Wave Motion* 46.7 (Nov. 2009), pp. 451–467.

[46] H. Ammari, E. Bretin, J. Garnier, and A. Wahab. “Time-Reversal Algorithms in Viscoelastic Media”. In: *European Journal of Applied Mathematics* 24.4 (Aug. 2013), pp. 565–600.

[47] B. E. Anderson, J. Douma, T. Ulrich, and R. Snieder. “Improving Spatio-Temporal Focusing and Source Reconstruction through Deconvolution”. In: *Wave Motion* 52 (Jan. 2015), pp. 151–159.

[48] M. Fink. “Time-Reversal Mirrors”. In: *Journal of Physics D: Applied Physics* 26 (1993), pp. 1333–1350.

[49] D. Givoli. “Time Reversal as a Computational Tool in Acoustics and Elastodynamics”. In: *Journal of Computational Acoustics* 22.03 (Sept. 2014), p. 1430001.

[50] A. Love. *A Treatise on the Mathematical Theory of Elasticity.* University Press, 1934.

[51] T. J. R. Hughes. *The Finite Element Method: Linear Static and Dynamic Finite Element Analysis.* Dover Publication, 2000.

[52] J. A. Cottrell, T. J. R. Hughes and Y. Bazilevs. *Isogeometric Analysis: Toward Integration of CAD and FEA*. Chichester, West Sussex, U.K. ; Hoboken, NJ: Wiley, 2009. 335 pp.

[53] R. Kolman, J. Plešek, M. Okrouhlík and D. Gabriel. “Grid Dispersion Analysis of Plane Square Biquadratic Serendipity Finite Elements in Transient Elastodynamics”. In: *International Journal for Numerical Methods in Engineering* 96.1 (2013), pp. 1–28.

[54] R. Kolman, J. Plešek, J. Červ, M. Okrouhlík and P. Pařík. “Temporal-Spatial Dispersion and Stability Analysis of Finite Element Method in Explicit Elastodynamics”. In: *International Journal for Numerical Methods in Engineering* 106.2 (2016), pp. 113–128.

[55] Y. Wang. “Frequencies of the Ricker Wavelet”. In: *GEOPHYSICS* 80.2 (2015), A31–A32.

[56] J. D. Achenbach. *Wave Propagation in Elastic Solids, by J. D. Achenbach.* North-Holland Pub. Co.; American Elsevier Pub. Co Amsterdam, New York, 1973, xiv, 425 p.